Chinese Journal of Aeronautics, (2015), 28(6): 1784–1792

Chinese Society of Aeronautics and Astronautics
& Beihang University

Chinese Journal of Aeronautics

cja@buaa.edu.cn
www.sciencedirect.com

Experimental investigation on impact performances of GLARE laminates

Chen Qi, Guan Zhidong *, Li Zengshan, Ji Zhaojie, Zhuo Yue

School of Aeronautic Science and Engineering, Beihang University, Beijing 100191, China

Received 28 January 2015; revised 2 March 2015; accepted 25 March 2015
Available online 29 August 2015

KEYWORDS

Concentrated quasi-static indentation force;
Delamination;
GLARE laminate;
Impact;
Indentation

Abstract An experimental investigation was carried out on the damage resistance to a concentrated quasi-static indentation force and low-velocity impact of four kinds of glass-reinforced aluminum laminates (GLARE for short). Compared with the experimental results of the CFRP (Carbon Fiber Reinforced Plastics) laminates, the performance of GLARE was determined. By means of concentrated quasi-static indentation force test, typical force–displacement response, the maximum contact force and dent depth were received. Through drop-weight low-velocity impact tests, impact force histories, indentation depths (through a new method) and dissipated energy were obtained. The test results show that the force–displacement response of GLARE 4 laminates under the concentrated quasi-static indentation force has an obvious flat roof and the failure is instantaneous, which are different from CFRP laminates. The indention will be visible once the impact happens. C-scan results find that there is no delamination besides the impact area after both the concentrated quasi-static indentation and low-velocity impact. The dissipated energy approximately equals the impact energy.

1. Introduction

GLARE (glass-reinforced aluminum laminate) is a new class of fiber metal laminates and it is also the culmination development working together by Delft University of Technology and the Netherlands National Aerospace Laboratory (NLR).[1,2] GLARE is a laminate' sets composed of alternating layers of 2024-T3 aluminum in 0.2–0.5 mm and S-2 glass-fiber reinforced bond film in 0.1–0.3 mm. After the process in autoclave, the laminate is completed. GLARE laminates can be tailored to suit a wide variety of applications by changing the fiber/resin system, the alloy type and thickness, stacking sequence, fiber orientation, surface pretreatment technique, and so on.[3]

GLARE has found a lot of applications by now. Experimental repair patches are applied for the C5 Galaxy of the US Air Force.[2] GLARE is selected for the Boeing 777 impact resistant bulk cargo floor.[4] While Airbus has chosen GLARE for A340–500/600 wing leading edge J-nose, A380–800 fuselage is the first large-scale application of GLARE. A380 incorporates 27 GLARE skin panels covering a total area of 469 m^2 in the upper fuselage skin, with further usage in the leading edges of both the horizontal and vertical tail planes.[1,5,6]

* Corresponding author. Tel.: +86 10 82338873.
E-mail address: zdguan@buaa.edu.cn (Z. Guan).

Peer review under responsibility of Editorial Committee of CJA.

Production and hosting by Elsevier

http://dx.doi.org/10.1016/j.cja.2015.07.002
1000-9361

Impact damage is unavoidable during the manufacture and flight of planes. There are several kinds of impact damages: Instruments falling on the floor, the shock of stones on the runway during the take-off and landing and hail and birds during flight. The damage which should be paid more attention to during composites structures' design is low-velocity impact. As the most important part of damage tolerance in composites structures, low-velocity impact is always the key and difficult point. There are a lot of researchers on tests, theoretical analysis and finite element analysis of low-velocity impact. It contains the impact response of structures and the mechanism of impact damage.[7–10] Vlot and Krull[4,11] performed static indentation and low and high velocity impact tests on three kinds of GLARE which had not been classified in 1996 and 1997. Vlot is the first one who studies the impact damage of GLARE. Laliberté et al.[12] carried out extensive series of impact on GLARE 3 2/1, 4 2/1 and 5 2/1 and considered three kinds of fixture in 2005. Wu et al.[6,13] investigated the impact properties and damage tolerance of GLARE 4 3/2 and 5 2/1, and the post-impact residual tensile strength under various damage states was also measured in 2007. What's more, scholars from China and other countries also do infinite studies in CAI in tests and theories.[5,14–19] There are also two detailed review papers on impact response of fiber metal laminates.[20,21]

Compared with aluminum laminate and composite materials, fiber metal laminate has the best impact property. In most cases, the metal laminate could absorb most of the impact energy. It is because the laminate forms visible indentions after impact that we could inspect the damage easily. One could refer to Ref.[6,22] about the classification of the GLARE. GLARE is classified into six categories and the content of fiber of GLARE 5 is higher than any others' of GLARE. And GLARE 5 is a kind of special laminate for impact.[23] Utilizing GLARE is a better solution to the difficulty that other objects do harm to the plane itself.[24]

To fully understand GLARE laminates' damage process under impact load, this paper is assumed to be the first part to study the mechanism of impact damage with the experiments. Further research has been carrying out considering the damage model through a finite element method based on the consideration of fiber failure, along with the comparison between the results of experiments and simulations, to have a better understanding on the impact damage mechanism of GLARE laminates.

2. Experimental

2.1. Materials

The GLARE laminates which are made in China in this article are a little different. We do not have the S-2 fiber now, so we take the S-4 instead and the thickness of S-4 glass-fiber reinforced bond film is 0.15 mm. The thickness of aluminium layer is 0.254 mm. These differences may result in some different characters of GLARE laminates between those made in China and other countries. The mechanical properties of 2024-T3 and S-4 glass-fiber reinforced bond film are shown in reference.[22,25]

Considering all the existing results,[6–13] no one has used ASTM composite standard test methods to study the properties of GLARE. To have a better contrast with composites, we applied ASTM standard test methods. Table 1 shows the laminates we chose. Specimens are 152 mm × 152 mm for quasi-static indentation test, and 150 mm × 100 mm in size is for low-velocity impact. The thickness of specimens is from 1.662 mm to 2.816 mm. Besides, graphite/epoxy composite materials (Carbon Fibre Reinforced Plastics, short for CFRP) are used for contrast. The CFRP laminate used here is T300/5228A, with its layup $[45/0/-45/90/-45/90/45/0]_s$, 2 mm in thicknesss, 25/50/25 in layup proportion.

Table 1 Average thickness and stacking sequence for specimens.

Group	Lay-up	Thickness (mm)
A	Al/0/90/0/Al/0/90/0/Al	1.662
B	Al/0/90/0/Al/0/90/0/Al/0/90/0/Al	2.366
C	Al/0/90/90/0/Al/0/90/90/0/Al	1.962
D	Al/0/90/90/0/Al/0/90/90/0/Al/0/90/90/0/Al	2.816

2.2. Procedure

The quasi-static indentation (QSI) test follows the "Standard test method for measuring the damage resistance of a fiber-reinforced polymer-matrix composite to a concentrated quasi-static indentation force".[26] Damage is imparted by an out-of-plane and concentrated force (perpendicular to the plane of the laminated plates) applied through slowly pressing a displacement-controlled hemispherical indenter into the face of the specimen. The testing machine WDW-200EIII comes from SHIDAISHIJIN, China. The diameter of hemispherical indenter is 12.7 mm. The fixture including a single plate with a (127.0 ± 2.5) mm diameter opened in the middle is made of steel. The size of the fixture is 200 mm × 200 mm × 40 mm.

The low-velocity impact testing follows the "Standard test method for measuring the damage resistance of a fiber-reinforced polymer matrix composite to a drop-weight impact event".[27] Test machine is designed by our advisor.[28] A guided drop weight tester was used for the impact tests in which an instrumented mass (impactor) drops from a specific height onto the center of the specimen held by a support. The supporting fixture for the specimens is a steel plate with a cutout of 125 mm × 75 mm in size. The impactor has a spherical head with a diameter of 16 mm and a mass of 5.36 kg. The impact energies vary from creating indentations with their depths from approximately zero to almost penetrating the laminate, thus forming a curve of the indentation depth – impact energy relationship. Data of force versus time is recorded during the contact. After the impact, indentation depth is measured through a new method immediately.

C-scan inspections were carried out to the specimens after tests to check the extent of delamination occurring in the laminates. All C-scan inspections are performed by using a GE USIP 40 flaw detector whose model is 1 MHz and the space of scan is 0.50 mm.

3. Results and discussion

3.1. QSI experiment results

Fig. 1 shows the typical QSI force–displacement responses of GLARE laminates and graphite/epoxy composite materials

(Carbon Fibre Reinforced Plastics, short for CFRP). From Fig. 1, we find a lot of differences between GLARE and CFRP laminates. The slope of CFRP is almost constant, and the two slopes of the two phases of the CFRP curve are nearly the same. Simultaneously, the slopes of GLARE are changing and lower than CFRP. The residual depth of CFRP is shorter than that of GLARE. The first failure is defined by the first discontinuous point of the force–displacement response. The load at the first failure point of GLARE is almost near the peak of the curves, while the one of CFRP laminates is only half of the peak. The first failure is the starting point of laminate's failure, moreover after the first failure, the load of CFRP laminate will keep on going up until the load reaches the peak load. The force–displacement responses of GLARE have a flat roof after the first failure, but CFRP has no such roof. The drop of GLARE force–displacement response is instantaneous, whereas the failure of CFRP is slow and progressive. Fig. 2 gives the indentations remaining in specimens. Indentations of Group A and Group B are like a diamond, cracks on the laminate look like a "+", while Group C and Group D are ellipse, and cracks on the laminate look like a fallen "I". The depth of indentations of GLARE is more than 4 mm. As we all know, the indentation left in CFRP is less than 3 mm and difficult to discover as shown in Fig. 2.

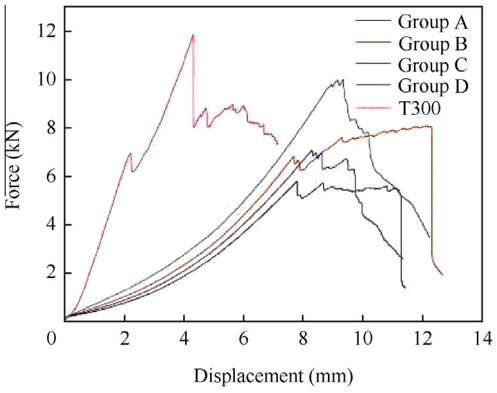

Fig. 1 Force–displacement responses of Group A, B, C, D and T300 specimens.

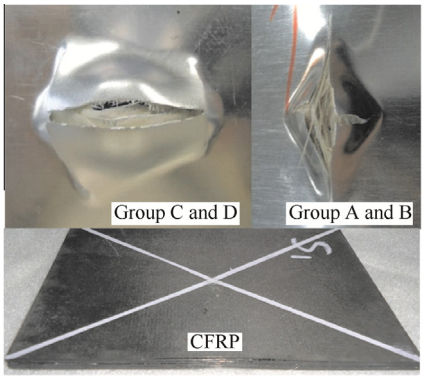

Fig. 2 Indentations of Group A, B, C, D and T300 specimens after removal of applied force.

From Fig. 1, the force–displacement responses of Group A and Group B are similar, while Group C resembles Group D in force–displacement responses, so the test results will be discussed from two parts. In the beginning, load rises along with the displacement rising till the first failure. This process shows that the damage resistance of GLARE is growing up with the displacement rising, while CFRP keeps a constant stiffness. The tensile modulus of T300 is 135 GPa, aluminum is 68 GPa and S-4 fiber is 52 GPa.[22,25] The whole tensile modulus of GLARE is much smaller than T300, so the slopes of GLARE are lower than CFRP. Furthermore, the thickness along the load direction is only about 2 mm and the fixture includes a single plate with a (127.0 ± 2.5) mm diameter open in the middle, the laminate has enough space to produce deformation to resist the load. When the aluminum plies come into the plastic stage, the whole tensile modulus of GLARE is changing, so the load–displacement curves are nonlinear. While the CFRP only has one type carbon fiber, the slope is constant. The long plastic stage and ultimate tensile strain result in a big hole (indention) after loading.

Fig. 3 shows the state of GLARE specimen under the load of about 5 kN for Group A and 6 kN for Group C which is before the first failure. The delamination between middle aluminum layer (A-2) and fiber layer (0-3) below it is found as shown in Figs. 3 and 4. First of all, the indenter is above layer A-1, so distances between layers and the indenter increase from top to bottom (from A-1 to A-3). When the indenter has a displacement, the displacements along 0° of different plies increase from top to bottom (from A-1 to A-3). There are two kinds of interfaces: (1) aluminum on the top of fiber (A-1 and 0-1, A-2 and 0-3), (2) fiber on the top of aluminum (0-2 and A-2, 0-4 and A-3). Because aluminum has a bigger

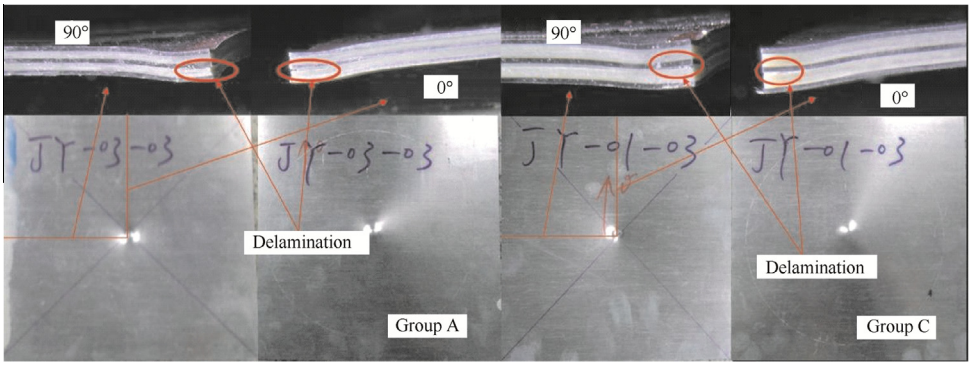

Fig. 3 Damage of Group A and C before first failure.

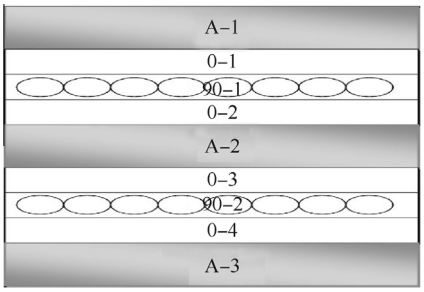

Fig. 4 Lay-up of Group A.

ultimate strain than glass fiber, when the load is carrying on, there must be transverse shear stress in the matrix. When fibers are on the top of aluminum (Interface 2), the strain is continuous between adjacent layers. As far as Interface 1, strains of adjacent layers are continuous when it is very small (like A-1 and 0-1), the strain of glass fiber (0-3) could not reach the strain of aluminum (A-2) above it when strain grows bigger, which means the transverse shear stress is big enough and transverse shear cracks of matrix cracks are formed, so delamination is formed. Laminates of different Groups have the same delamination position (between A-2 and 0-3) because of different ultimate strains between aluminum and glass fiber. Moreover, clear indentions can be seen on both sides of the laminates by the naked eye at this moment.

Loading goes on. The first failure of CFRP is the time when the laminate has its first delamination. The delamination reduces the thickness of laminate and then reduces the bending stiffness of CFRP laminates, so the curve drops until the delamination around the indenter is pressed to no gap between adjacent plies by the indenter. The load will go on increasing until fiber breaks. During this process, delamination is expanding until fiber breaks. As shown in Fig. 3, delamination is already found before the first failure, so the first failure of GLARE is fiber break. The ultimate strength of CFRP is defined by fiber break. After the ultimate strength, new delamination does occur between 0-4 and A-3 (Interface 2), which has something to do with the transverse shear stress as Figs. 3 and 4 show. After the test, we find the two kinds of Interfaces have delamination. Only a few transverse shear cracks of matrix cracks can be seen between fibers around the break. Delamination in Interface 1 and 2 and fiber break on both directions give enough space for the indenter, which explains why the delamination area is much smaller than CFRP. As Figs. 5 and 6 show, delamination of GLARE is inside the deformation which can be seen by eyes easily through section pictures, which is different from the CFRP laminates.[29] According to Fig. 6 C-scan results, inter delamination of GLARE laminates is only in the area of visible deformation, which also proves that the delamination is detectable by eyes. The only job needing to do to confirm the failure inside the laminate is measuring the area of the intention. Through

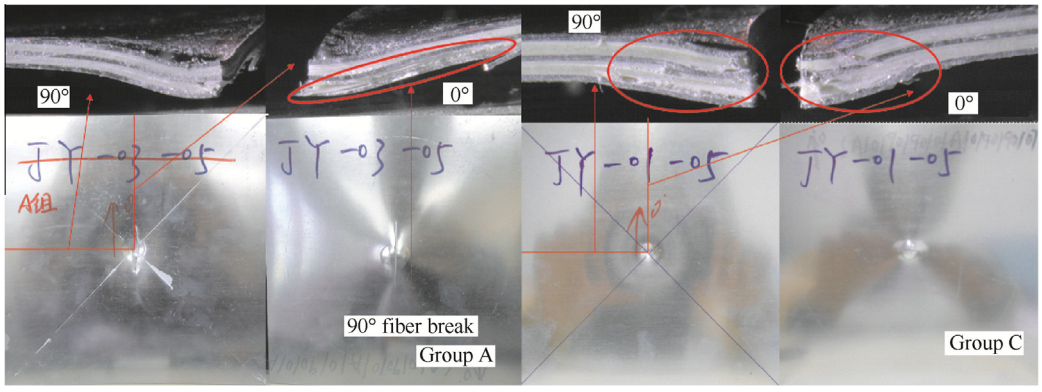

Fig. 5 Damage of Group A and C after ultimate strength.

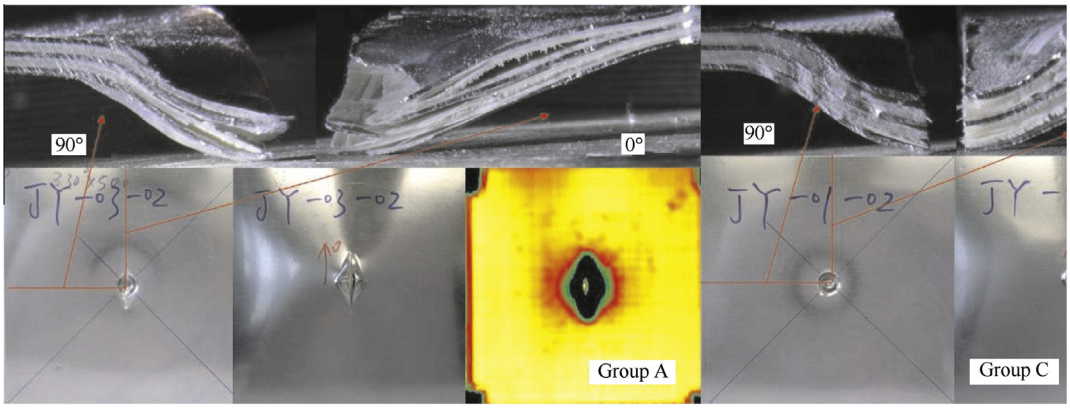

Fig. 6 Damage of Group A and C after the experiment.

Fig. 1, when the type of GLARE is fixed, the first failure is determined by the thickness of laminate. When the number of aluminum plies is fixed, the first failure is determined by the type of GLARE.

The specific elongation of Al is 19%, and the one of S-4 fiber is only 4%. After the aluminum gets into the plastic stage and the delamination happens, there will be a long time when the fiber is the main element bearing the load. Moreover, the fiber content of two directions is not equal. As Fig. 5 Group A shows, there is only a few fiber break along 0 degree, while there is a large number of fiber break along 90°. When the fiber of 90° breaks completely, the aluminum ply has a crack whose direction is perpendicular to 90°, which can prove the 90° fiber break outside the laminate. Subsequently, the fiber of 0° will take the load until all the fiber near the indenter is broken. And the quantity of fiber in 0° is twice as big as that in 90°. That is why the force–displacement responses of Group A and Group B have a flat roof. When it comes to Group C and Group D, the content of fibers in the 0° equals that in 90° direction. Fibers of both directions take the load together, and there is no load transmit from 90° to 0° fiber like Group A and Group B, so with the increase of load, the 0° direction fiber ply (0-4 in Fig. 4) in the non-impact side fractures firstly. Clear sound of fiber fracture can be heard during the experiment. After that, the aluminum in the non-impact side is pulled off. The fiber breaks from non-impact side to the impact side while the load descends, so the force–displacement responses of Group C and Group D have no such flat roof as Group A and Group B. The ultimate strength of GLARE laminates is defined by fiber break, so is the initial failure load at the first failure. Therefore the first failure and the ultimate strength of GLARE are very close.

The drop of GLARE force–displacement response is instantaneous, because the failure of the whole laminate of Group A and Group B is determined by 0° fiber break. The fiber break of 0° is instantaneous, so is the response. Finally, a cross-shaped crack is obtained as shown in Fig. 2 and the specimen is punctured. With regard to Group C and Group D, the displacement of the indenter increases due to the continuous fiber fracture in the laminate. Finally, aluminum ply in the non-impact side of outermost layer of the laminate appears a fallen I-shaped crack as shown in Fig. 2 which is different from Group A and Group B. The complete failure of the laminate in Group C and Group D is a gradual process.

For Group A and Group B, the content ratio of fiber in both directions is 2:1, so the strength ratio on both sides is 2:1. The strength along 0 degree is twice as big as 90°, so the length of crack along 90° is only half of the length of crack along 0°. Because of the strength weakness along 90°, fibers along 90° break firstly, so there is a crack along 0°. When the break along 90° does not meet the indenter's displacement need, fibers on 0° begins to break. So new cracks emerge at the point which has the biggest placement. This is how the diamond and "+" cracks formed. For Group C and Group D, the fiber contents equal with each other, so the fiber breaks from the non-impact side to the impact side. The direction of fiber breaks firstly is 0° on the non-impact side, so there is a long crack along 90°. And the crack is clear and neat. When the fiber and aluminum break later, the indenter has a large displacement. The break on 90° is not that regular as 0°, but they are all in the impact area. So cracks on non-impact side along 90° move to the edge of impact area. The aluminum around crack tips is pulled by the indenter, then there are two cracks vertical to the first one. This is how the ellipse and fallen "I" formed.

3.2. Low-velocity impact test results

Low-velocity impact is well worth noticing in composite structure design. It is because that residual strength of composite laminates with low-velocity impact damage reduces by 60% at most and the internal damage cannot be detected easily in composite laminates with low-velocity impact damage. Indention depth, the impact of contact force–time curve, damage area and impact energy dissipation are used to describe the impact damage resistance of materials. These variables will be discussed in the analysis of the results of low-velocity impact test.

3.2.1. Indention results

Permanent indention under the low-velocity impact is commonly used to describe the damage detection nature and the severity of the damage, which is the first concern in composite material design. The indention depth – impact energy responses of four kinds of GLARE laminates and T300 are shown in Fig. 7. GLARE test specimens have monolithic deformation while CFRP still keeps flat after impact, so the indention depth of Fig. 7 is not measured by the dial gauge, but by the new way as Fig. 8 shows. This new method overcomes the influence of the monolithic deformation, so we can focus on the indention caused by the impactor. First, we need a by using the vernier caliper during the text. a is the

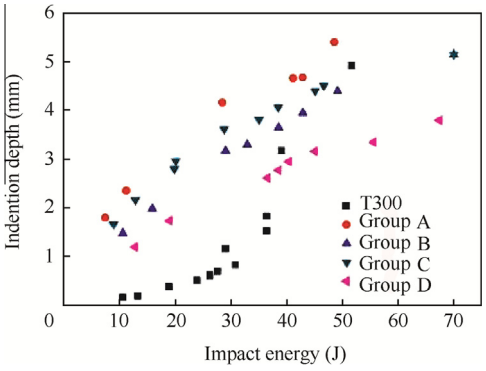

Fig. 7 Indentation depth – impact energy relationships of Group A, B, C, D and T300 specimens.

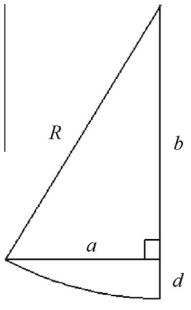

Fig. 8 Calculation method of indentation depth.

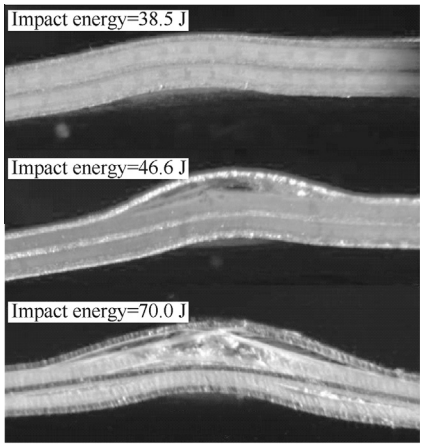

Fig. 9 Damage states of different energy of Group C.

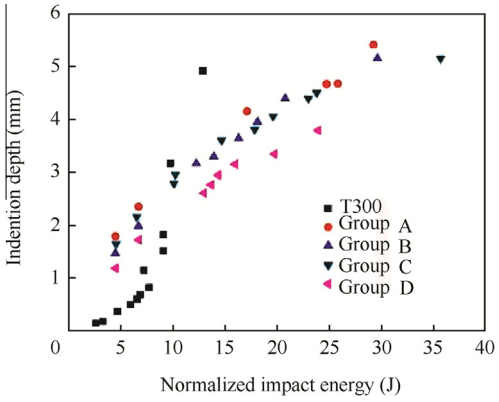

Fig. 10 Indentation depth – normalized impact energy relationships of Group A, B, C, D and T300 specimens.

radius of indentions (also the semi-minor axis of the indention if the indention is ellipse). R is the radius of the impactor. And according to the Pythagorean Theorem, we can get b,

$$b = \sqrt{R^2 - a^2} \tag{1}$$

And then d is obtained which is the new indention depth.

$$d = R - b \tag{2}$$

As we can see from Fig. 7, indention depths of each group increase with the rise of impact energy. The relationship of GLARE between indention depth and impact energy is almost linear, while the one of T300 is not. Ref. [30] proposed that there is an obvious inflection phenomenon in the indention depth-impact energy response of a low-velocity impact test on composite plates such as T300 in Fig. 7, and the slope increases after some knee point. Shen et al. considered that the knee point indicates the resistance change of composite laminate to a drop-weight impact. Before the knee point, fiber and resin have taken the impact load together; after the knee point, fiber breaks and the resistance decreases heavily, so the indention depth increases rapidly. Fig. 9 shows couple of pictures during the damage process of GLARE. Taking Group C for example, the laminate of Group C only has deformation until 38.5 J, at 46.6 J it has fiber break (0–4 in Fig. 4) and delamination (between 0–4 and A-3 in Fig. 4) at the non-impacted side. And at about 70 J the aluminum at the non-impacted side (A-3 in Fig. 4) has crack along 90 degree and the fiber (between A-3 and A-2 in Fig. 4) all breaks, while T300 has already penetrated at 50 J. The whole indention depth – impact energy response of Group C is almost linear. As we can see from Fig. 9, after the impact, the aluminum plies have very big plastic deformation, from which the aluminum plies absorb a great deal of energy, thereby protecting the glass fiber from breaking, so the fiber does not break until 46.6 J. To get rid of the influence of thickness, Fig. 10 shows indention

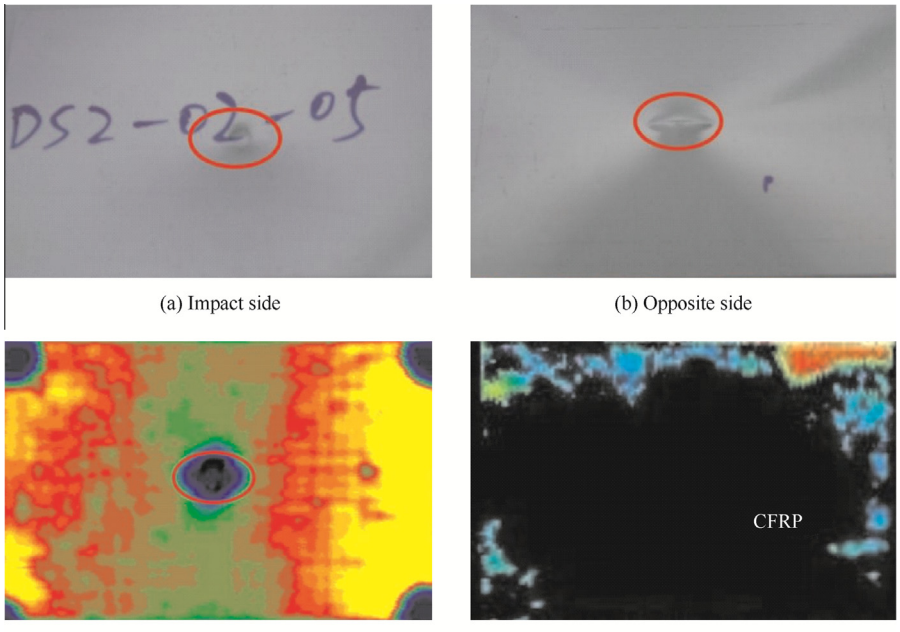

(a) Impact side (b) Opposite side

(c) C-scan result of GLARE specimen (d) C-scan result of T300

Fig. 11 C-scan images contrast between GLARE and CFRP specimens.

depth – normalized impact energy response. And the normalized impact energy equals the impact energy divided by thickness. As we can see the regularization results have the same trend as Fig. 7. All results show that an obvious inflection phenomenon in the indention depth-impact energy response of a low-velocity impact test on composite plates proposed in Reference[30] cannot be applied to GLARE laminates (fiber metal laminates). Besides, Fig. 10 also indicates that energy to have the same indention depth is not in proportion to the laminate thickness; the bigger the thickness is, the more the normalized impact energy to have the same indention depth is.

3.2.2. Delamination and C-scan results

The invisible delamination damage inside of the laminates can lead to residual strength reduction by 60% of composite laminates with low-velocity impact damage, which decreases the structure load capacity. The initial delamination damage reflects the resistance to delamination of composite material laminates. Fig. 11 shows the C-scan results of Group B at 49 J. And at the bottom there is a C-scan result of CFRP with the same energy. As you can see from Fig. 11, the delamination damage inside the laminates exists in visible deformed areas after low-velocity impact in GLARE laminates while it appears in larger areas inside of CFRP laminates; Reference[7] finds the same phenomenon. It is shown in blue and black areas inside the laminates in Fig. 11, which is similar to the results after the concentrated quasi-static indentation and the results in reference.[2] In Fig. 11, the blue areas in the corners of the laminate represent the gaskets which have no effects on laminate abilities. The deformation of laminates leads to changes of ultrasonic frequency, so there are green and red areas in the laminate.

Composite material structural damage was classified in composite structure design. Barely Visible Impact Damage, short for BVID, is needed to focus on what needs to be tested by professional equipment in order to be found in time, because it means further dangerous will happen on composite structure. Reference[31] pointed out that the indention depth for BVID is 1 mm. Considering all the results about indention, delamination and C-scan, there is no need to use complex equipment to detect GLARE structure damage, which is very convenient, because the indention will be visible once the impact happens and there is no delamination besides the impact area after both the concentrated quasi-static indentation and low-velocity impact.

3.2.3. Force–time response results

Contact force–time response curves under the impact energy levels 11, 20, 30, 40 J of the four kinds of GLARE laminates are shown in Fig. 12. Force–time responses got the same results with delamination and C-scan results, which is that there is no significant fluctuation when the impact energy is

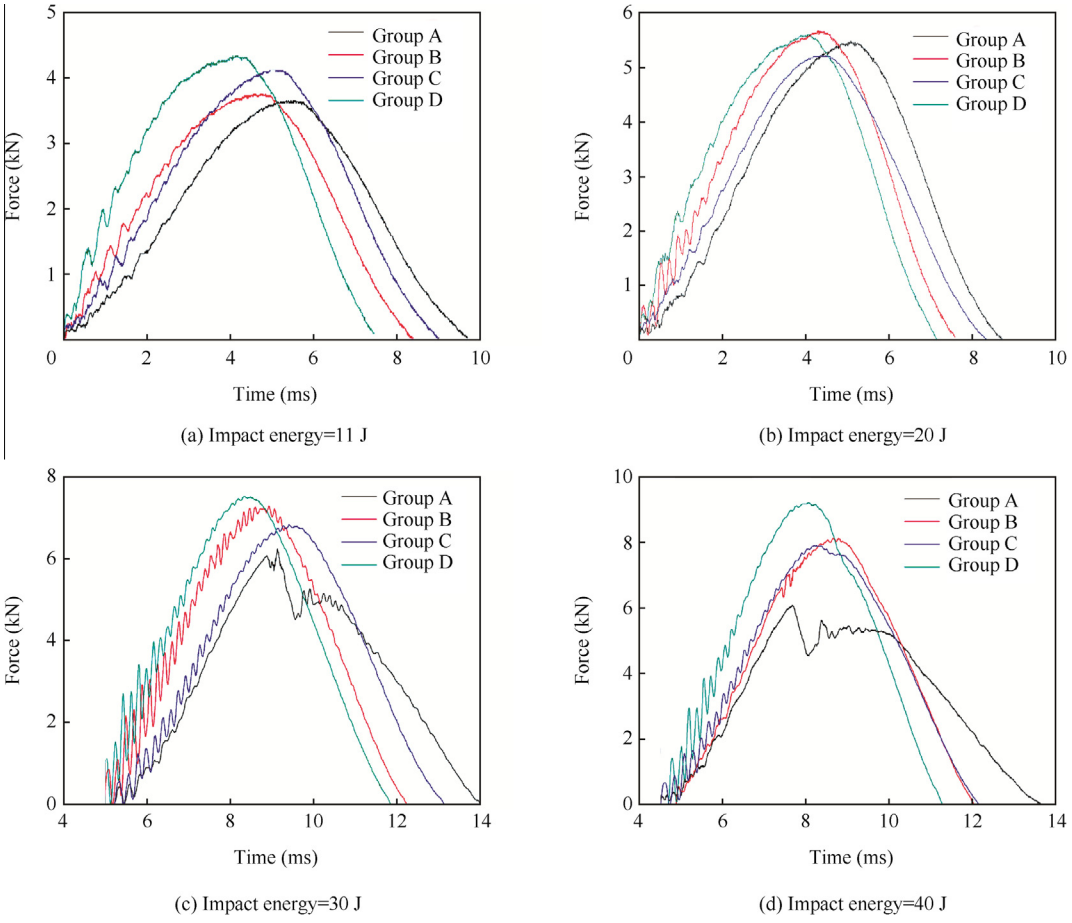

Fig. 12 Impact force versus time history of Group A, B, C and D.

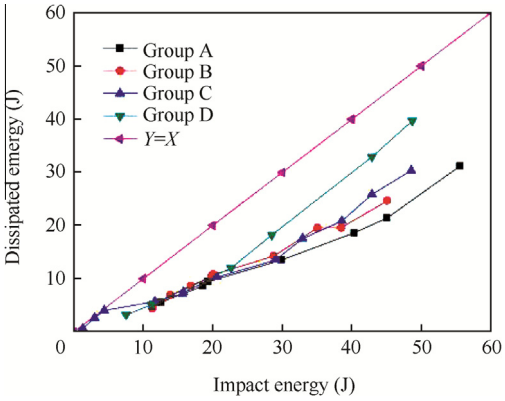

Fig. 13 Energy Profile Diagram of Group A, B, C and D.

under 40 J except Group A. The response of Group A becomes discontinuous between 22 J and 25 J, which is the sign of fiber break. Responses of other groups keep smooth under 40 J, which is also proved by Fig. 9. Because of the restriction of test condition, we did not perform the test above 50 J.

3.2.4. Energy profile diagram analysis

The actual impact energy and the energy of the rebounded indenter are deduced by the instantaneous impact velocity and rebound velocity which is measured on the speed measuring device of the impact test system. The Energy Profile Diagram (EPD for short) which is the reflection of dissipation of energy and impact energy, is used to analyze the energy dissipation. Energy Profile Diagrams of the impact test are shown in Fig. 13.

When the impact energy is less than 5 J, the energy dissipation is almost similar to the impact energy. That is to say, the impact energy is absorbed totally by the laminates, which differs from the Energy Profile Diagram of common composite materials in reference.[32] Due to the deformation of aluminum, the impact energy is absorbed. As the impact energy continued to rise, it is beyond the aluminum plate's capacity to absorb the energy with the plastic deformation, which can be seen that the indenter is bounced in the vertical direction. According to the conversation of energy, at the moment the indenter touched the laminate, the kinetic energy transforms into two parts as the dissipative energy and rebound kinetic energy of the indenter. When the impact energy varies between 10 J and 20 J, few differences exist in the dissipative energy of the four different laminates and the curves are much the same. When the impact energy is over 20 J, obvious differences begin to emerge. The dissipative energy ranks A–C–B–D in a descending order when the impact energy is between 20 J and 30 J, which suggests that the dissipative relates to the thickness of the laminate at this interval. When the impact energy is between 30 J and 40 J, Group B coincides with Group C. As the impact energy is over 40 J, the descending order of the dissipative energy changes to A–B–C–D. Distinct discrepancy comes into being between the dissipative energy of the GLARE 5 and GLARE 4, the dissipative energy of GLARE 5 is smaller than that in GLARE 4 and of the same kind of laminates; the thinner the laminate is, the higher the dissipative energy, and vice versa.

4. Conclusions

In this paper, the damage resistance to a concentrated quasi-static indentation force and low-velocity impact of four kinds glass-reinforced aluminum laminates has been studied. According to results in our work and Refs.[2–6,11–13], fibers made in China and abroad did not influence the damage resistance to a concentrated quasi-static indentation force and low-velocity impact of four kinds GLARE laminates. ASTM (American Society for Testing and Materials) are well accepted around the materials world, and its standard test methods of composite ASTM D 6264/D 6264 M – 07 and ASTM D 7136 /D 7136 M – 07 are also suitable for GLARE which is a new kind of fiber metal laminates. But not all classical conclusions of composites can be applied to GLARE laminates (perhaps fiber metal laminates).

The existence of aluminum has changed the QSI force–displacement responses' loading process into a nonlinear one. Fiber content in both directions decides the QSI force–displacement responses' shape (a flat roof and an instantaneous drop), moreover the indentions' shape and the cracks' distribution are also resolved by fiber contents in both directions.

The elasticity of aluminum makes the inspection more easier, because there will be an indention which can be seen by eyes clearly once the impact happens no matter how much the impact energy is. A new method to obtain the indention depth is invented to overcome the influence of the monolithic deformation. Delamination initiation load is not so important for GLARE, because all the delamination will be located within the deformation area. The existence of aluminum also promotes the damage resistance capacity to the impact according to the force–time response results and energy profile diagram.

References

1. Vogelesang LB, Vlot A. Development of fibre metal laminates for advanced aerospace structures. *J Mater Process Tech* 2000;**103**(1):1–5.
2. Gunnink JW, Volt A, de Vries TJ, Der Hoeven W. Glare technology development 1997–2000. *Appl Compos Mater* 2002;**9**:201–19.
3. Vlot A, Vogelesang LB, de Vries TF. Towards application of fibre metal laminates in large aircraft. *Aircr Eng Aerosp Tech* 1999;**71**(6):558–70.
4. Volt A. Impact loading on fibre metal laminates. *Int J Impact Eng* 1996;**18**(3):291–307.
5. Sinke J. Development of fibre metal laminates: concurrent multi-scale modeling and testing. *J Mater Sci* 2006;**41**(20):6777–88.
6. Wu GC, Yang JM. The mechanical behavior of GLARE laminates for aircraft structures. *JOM* 2005;**57**(1):72–9.
7. Choi HY, Chang FK. A model for predicting damage in graphite/epoxy laminated composites resulting from low-velocity point impact. *J Compos Mater* 1992;**26**(14):2134–68.
8. Gao D, Olsson R. *Impact on composite structures*. Cambridge: Cambridge University Press; 2004. p. 541–63.
9. Moura M, Gonçalves J. Modeling the interaction between matrix cracking and delamination in carbon–epoxy laminates under low velocity impact. *Compos Sci Technol* 2004;**64**(7–8):1021–7.
10. Guan Z, Yang C. Low-velocity impact and damage process of composite laminates. *J Compos Mater* 2002;**36**(7):851–71.
11. Volt A, Krull M. Impact damage resistance of various fibre metal laminates. *J Phys Iv France* 1997;**7**(C3), C3-1046-50.

12. Laliberté J, Stranznicky PV, Poon C. Impact damage in fiber metal laminates. Part 1: experiment. *AIAA J* 2005;**43**(11):2445–53.
13. Wu GC, Yang JM, Hahn HT. The impact properties and damage tolerance and of bi-directionally reinforced fiber metal laminates. *J Mater Sci* 2007;**42**(3):948–57.
14. Lin Z, Xu X. Residual compressive strength of composite laminates after low-velocity impact. *Acta Materiae Compositae Sin* 2008;**25**(1):140–6 Chinese.
15. Yang Y, Sun X, Yang S, Shen Z, Chai Y. Experimental study on compressive failure mechanism of low-velocity-impact-damaged composite laminates. *Acta Materiae Compositae Sin* 2012;**29**(3):197–202 Chinese.
16. Suemasu H, Ichiki M, Sameshima H, Nagashima T, Aoki Y. On compressive behavior and damage growth of impact damaged composite laminates. *9th China–Japan joint conference on composite materials*; 2010 Sep 16; Huhhot, China; 2010. p. 1–8.
17. Cesari F, Dal Re V, Minak G, Zucchelli A. Damage and residual strength of laminated carbon–epoxy composite circular plates loaded at the centre. *Compos Part Aappl S* 2007;**38**(4):1163–73.
18. Moriniere FD, Alderliesten RC, Benedictus R. Low-velocity impact energy partition in GLARE. *Mech Mater* 2013;**66**:59–68.
19. Tsamasphyros GJ, Bikakis GS. Analytical modeling to predict the low velocity impact response of circular GLARE fiber-metal laminates. *Aerosp Sci Technol* 2013;**29**(1):28–36.
20. Sadighi M, Alderliesten RC, Benedictus R. Impact resistance of fiber-metal laminates: a review. *Int J Impact Eng* 2012;**49**:77–90.
21. Chai GB, Manikandan P. Low velocity impact response of fibre-metal laminates – a review. *Comp Struct* 2014;**107**:363–81.
22. Chen Q, Guan ZD, Li ZS. Review of GLARE technology development. *Sci Technol Rev* 2013;**7**:50–6 Chinese.
23. Vermeeren CAJR. An historic overview of the development of fiber metal laminates. *Appl Compos Mater* 2003;**10**:189–205.
24. Yang NB, Liang W. *Introduction to composite structural design for large aircraft*. Beijing: China Aviation Publishing & Media Co., Ltd.; 2009. p. 105–7 Chinese.
25. Chen Q, Guan ZD, He W, Zhang M. An investigation on the tensile behavior of glass-reinforced aluminium laminate. *AIAA modeling and simulation technologies conference*; 2013 Aug 19–22; Boston, Massachusetts, USA; 2013.
26. American Society for Testing and Materials. Standard test method for measuring the damage resistance of a fiber-reinforced polymer-matrix composite to a concentrated quasi-static indentation force; 2007. Report No.: ASTM D 6264/D 6264M–07.
27. American Society for Testing and Materials. Standard test method for measuring the damage resistance of a fiber-reinforced polymer matrix composite to a drop-weight impact event; 2007. Report No.: ASTM D 7136/D 7136M–07.
28. Guan ZD, Zhao W. FC impact testing machine and the research of low velocity impact damage of T300/QY8911 composite plates. *Acta Materiae Compositae Sin* 2005;**22**(12):27–31 Chinese.
29. Guan ZD, He W, Chen JH, Liu L. Permanent indention and damage creation of laminates with different composite system. *Plym Compos* 2013;**35**(5):872–83.
30. Chen P, Shen Z, Xiong J, Yang S, Fu S, Ye L. Failure mechanisms of laminated composites subjected to static indentation. *Compos Struct* 2006;**75**(1–4):489–95.
31. Shen Z, Yang S, Chen P. Experimental study on the behavior and characterization methods of composite laminates to withstand impact. *Acta Materiae Compositae Sin* 2008;**25**(5):125–33 Chinese.
32. Aktas M, Atas C, Murat İçten B, Karakuzu R. An experimental investigation of the impact response of composite laminates. *Compos Struct* 2009;**87**(4):307–13.

Chen Qi is a Ph. D. candidate at School of Aeronautic Science and Engineering, Beihang University. Her area of research includes composite structures design and composite damage simulation.

Guan Zhidong is a professor and Ph. D. supervisor at School of Aeronautic Science and Engineering, Beihang University. His current research interests are composite damage tolerance, composite repair and composite design.